

Electronic Supplementary Information for

A New Strategy to Fabricate Composite Thin Films with Tunable Micro- and Nanostructures via Self-Assembly of Block Copolymers

Xingjuan Zhao,^a Qian Wang,^a Yong-Ill Lee,^b Xiao Chen,^a Jingcheng Hao,^a and Hong-Guo Liu^{*a}

^a Key Laboratory for Colloid and Interface Chemistry of Education Ministry, Shandong University, Jinan 250100, P. R. China. E-mail: hgliu@sdu.edu.cn;

^b Anastro Laboratory, Department of Chemistry, Changwon National University, Changwon 641-773, Korea

1. Experimental Section

1.1. Chemicals

The homopolymer P2VP with a M_n value of 5300 (denoted as P0) and block copolymer PS-*b*-P2VP with two blocks with M values of 7500/12500 ($M_w/M_n = 1.06$, P1), 30000/12500 ($M_w/M_n = 1.06$, P2), 110000/12500 ($M_w/M_n = 1.09$, P3), and 440000/20000 ($M_w/M_n = 1.2$, P4) were purchased from Polymer Source (Canada) and used as received. DMF ($\geq 99.5\%$) was obtained from Sinopharm Chemical Reagent Co. Ltd. (Shanghai, China), and used as received. Chloroform (analytical reagent) containing 0.3–1.0% ethanol as a stabilizer was obtained from Tianjin Guangcheng Chem. Co. The water used was highly purified using a UP water purification system (UPHW-IV-90T, Chengdu China) with a resistivity $\geq 18.0 \text{ M } \Omega \text{ cm}$. KBH_4 ($\geq 97.0\%$) and AgNO_3 (99+%) were purchased from Zhanyun Chem. Co. Ltd. and Shanghai Chemical Plant, respectively. 4-Nitrophenol (4-NP) (analytical reagent) was supplied by Tianjin Guangfu Fine Chemical Research Institute.

1.2. Preparation of freestanding films

First, a certain amount of PS-*b*-P2VP or P2VP was dissolved in DMF, and then a certain amount of CHCl_3 was added to form a mixed solution. In a typical experiment, about 5 mL of polymer solution ($V_{\text{DMF}}/V_{\text{CHCl}_3} = 6/4$) with 0.2 mg mL^{-1} P3 was poured into a clean and dry bottle with a diameter of 3.5 cm. Then, an equal volume of an aqueous solution of Ag^+ (0.01 mol L^{-1})

was added slowly and carefully by pipet along the bottle wall to cover the organic solution. A clear planar liquid/liquid interface was formed. The organic and aqueous phases are referred to as the lower and upper phases, respectively. A mass transfer process occurred immediately as soon as the interface formed, with a thin film rapidly appearing at the air/liquid interface. In the various control experiments, only one experimental parameter was changed, in contrast with the typical experimental conditions mentioned above. For example, to investigate the influence of the concentration of Ag^+ on the film formation and structure, the other parameters, including the volume ratio of DMF to CHCl_3 (6/4), the concentration of P3 (0.2 mg mL^{-1}), and the volume ratio of the organic and to aqueous solution (5 mL/5 mL) remained consistent with the typical experiment.

1.3. Catalytic reaction

In order to reduce the Ag^+ ions that doped in the as-prepared composite film completely, the film adhered to a frame was immersed into a KBH_4 aqueous solution with a concentration of 0.02 mol L^{-1} for about 30 mins and then washed with deionized water. This film was used as catalyst.

About 0.5 mL of an aqueous solution of 4-NP with a concentration of $2 \times 10^{-4} \text{ mol L}^{-1}$ was poured into a 1 cm quartz cuvette, after which 1.0 mL of an aqueous solution of KBH_4 with a concentration of $2 \times 10^{-2} \text{ mol L}^{-1}$ was added. Subsequently, the pre-treated thin composite film adhered on a frame was immersed vertically in the reaction system to catalyze the reduction of 4-NP to 4-aminophenol (4-AP). The progress of the reaction was monitored by using a UV-vis spectrometer (HP 8453E). The reaction temperature was maintained at 25, 30, 35, and 40 °C by a thermostat.

1.4. General characterization

The morphology and structure of the untreated and treated thin films deposited on copper grids were investigated using high-resolution transmission electron microscopy (HRTEM, JEOL-2010) with an accelerating voltage of 200 kV. The compositions of these samples were probed using X-ray photoelectron spectroscopy (XPS, ESCALAB MKII) with an $\text{Mg K}\alpha$ exciting source at a pressure of $1.0 \times 10^{-6} \text{ Pa}$ and a resolution of 1.00 eV. Field emission scanning electron microscopy (FESEM, Model JSM-7600F, JEOL Ltd., Tokyo, Japan) was used to characterize the

morphologies of the composite films. UV-vis spectra were obtained using a UV-vis spectrophotometer (HP, 8453E).

1.5. Dynamic light scattering (DLS) measurement

In order to observe the process by which the composite film was formed, the upper phase was monitored using the DLS technique with a BI-200SM research goniometer and laser light scattering system (Brookhaven Instruments Corporation). Measurements were carried out with a scattering angle of 90° at room temperature.

2. Additional figures

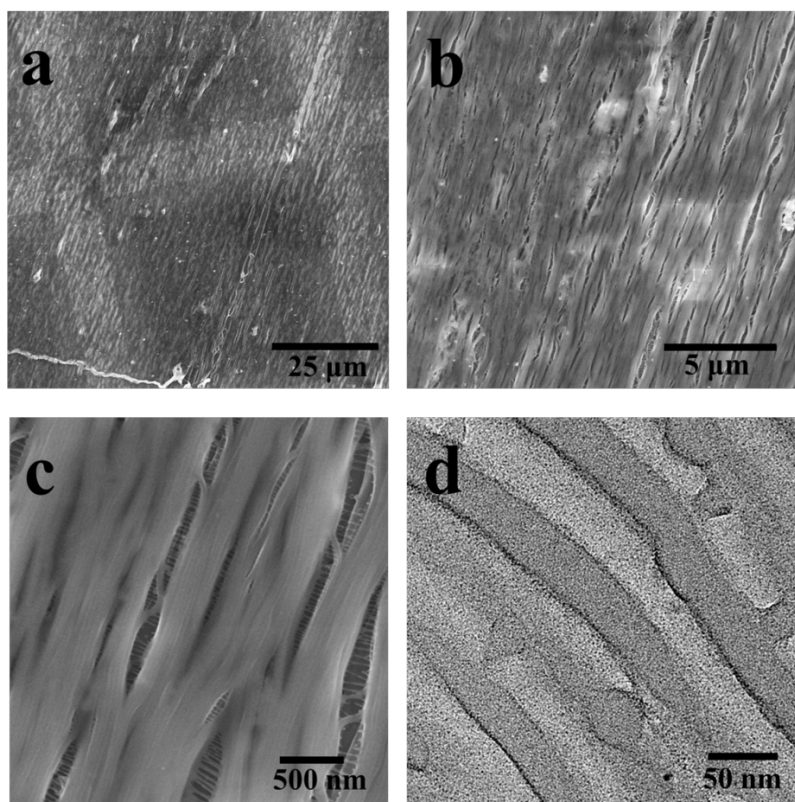


Fig. S1. Micrographs of composite thin films of block copolymer P3 formed at the air/water interface under typical experimental conditions: (a, b and c) SEM images of the film obtained after 20 h; (d) TEM image of the film obtained after 8 h.

Large-scale nanowire arrays formed in the film and bundles of nanowires appeared with time. In addition, it can clearly be seen in Fig. S1d that, besides the nanowires, nanospheres appear, with a large amount of nanoclusters distributed on the surface of the nanowires and nanospheres. The nanoclusters are thought to be the result of the reduction of Ag^+ ions by DMF during the assembly process.

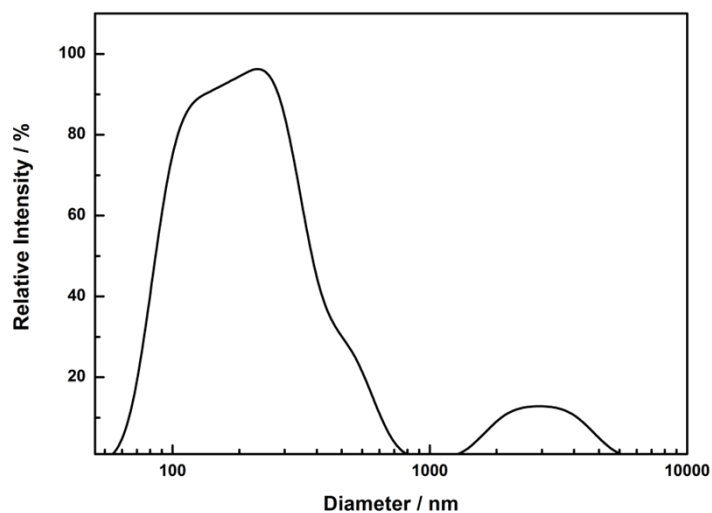


Fig. S2. DLS results of the upper phase (aqueous solution) observed after 5 min.

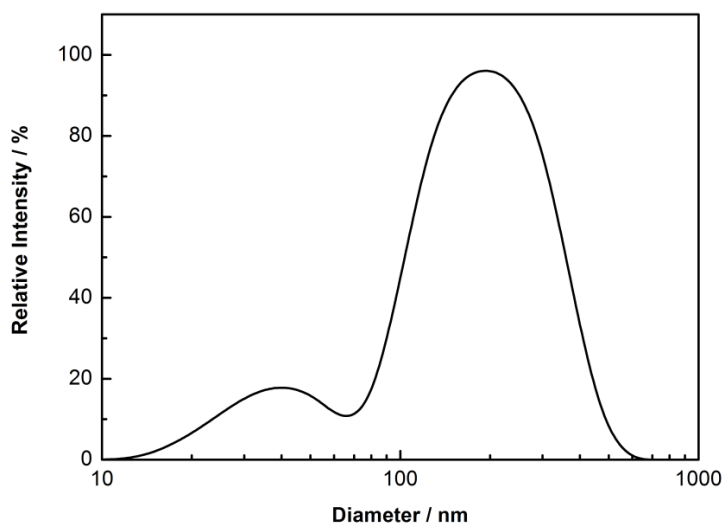


Fig. S3. DLS results of the upper phase (aqueous solution) observed after 8 h.

After the DMF molecules diffused into the water, large particles with a size of several micrometers formed and then disappeared quickly. These particles are likely to be droplets. The aggregates with the size of several tens of nanometers and several hundreds of nanometers are probably spherical and cylindrical micelles. This data is in agreement with the TEM investigation.

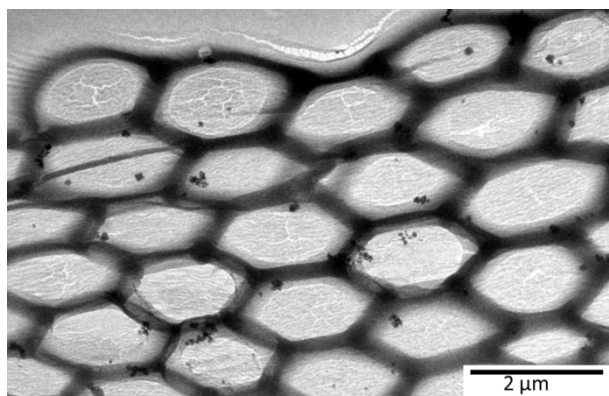


Fig. S4. A TEM micrograph of a composite thin film of P3/Ag. The volumes of the aqueous solution and the organic phase are both 5 mL, $V_{\text{DMF}}/V_{\text{CHCl}_3} = 6/4$, and the concentrations of P3 and Ag^+ are 0.2 mg mL^{-1} and 0.008 mol L^{-1} , respectively.

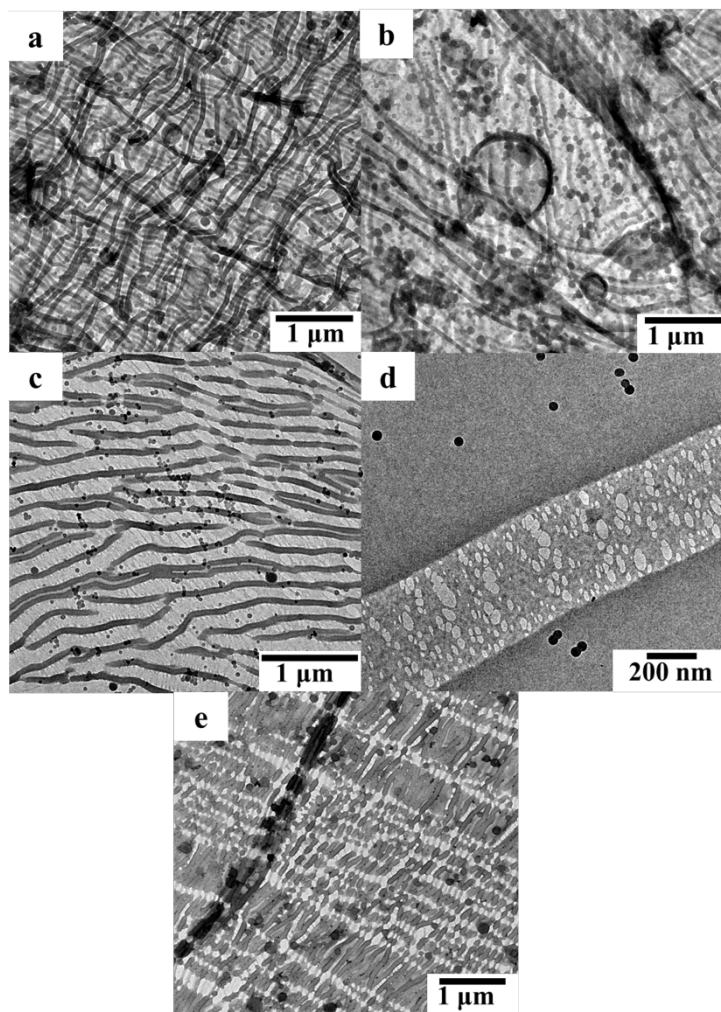


Fig. S5. TEM micrographs of thin films formed at the air/water interface with a P3 concentration of 0.4 mg mL^{-1} (a, b) and 0.1 mg mL^{-1} (c, d, and e), respectively. The volumes of the aqueous solution and the organic phase are both 5 mL, $V_{\text{DMF}}/V_{\text{CHCl}_3} = 6/4$, and the AgNO_3 concentration is 0.01 mol L^{-1} .

The PS-*b*-P2VP concentration also affects the formation of microstructures. As seen in Fig. S5a and b, large numbers of less-ordered nanowires, nanospheres, and hollow spheres appeared at the interface of a 0.4 mg mL^{-1} solution of P3. With the P3 concentration decreasing to 0.1 mg mL^{-1} , sparse and short nanowires appeared, which, despite their similar orientation, display non-uniform interval spacing larger than that of the nanowires that formed when a 0.2 mg mL^{-1} solution was used (Fig. S5c). Meanwhile, ellipsoids, and nanorods assembled into the incomplete

1D structures (Fig. S5e). In addition, cracks and holes appeared in the Gibbs adsorption background film due to the reduced availability of PS-b-P2VP molecules (Fig. S5d).

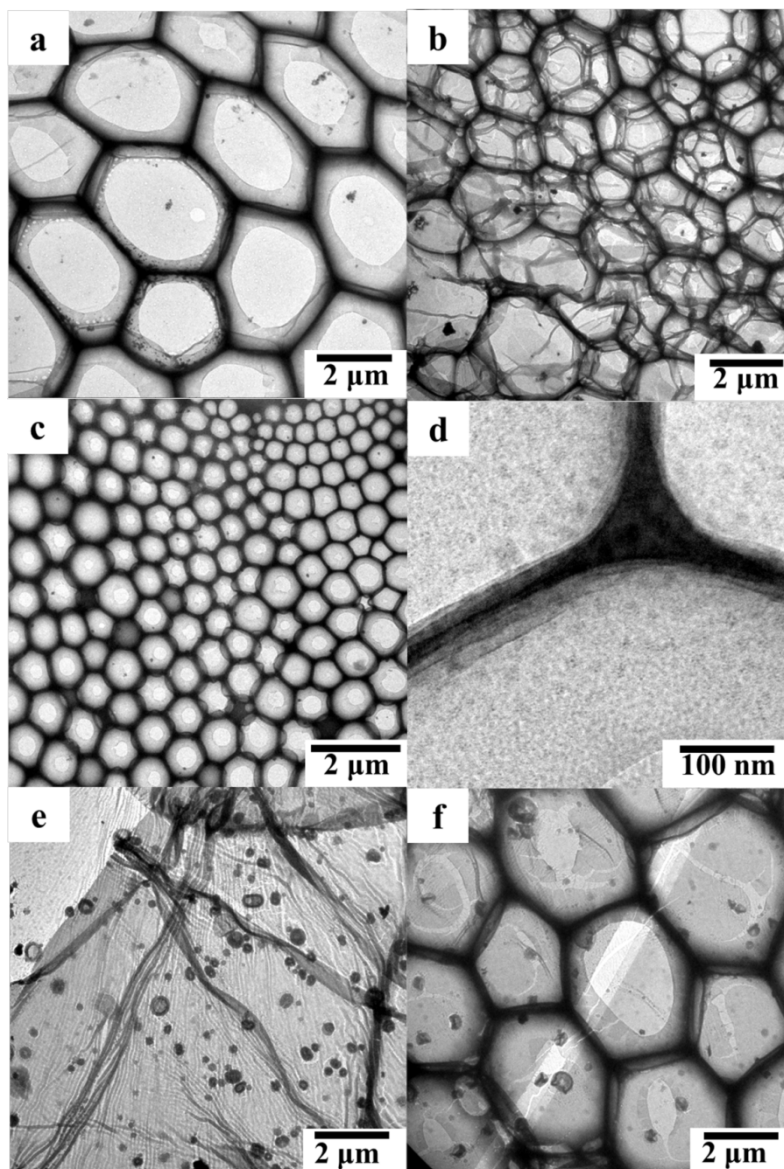


Fig. S6. TEM micrographs of thin films formed at the air/water interface: (a) $V_{\text{DMF}}/V_{\text{CHCl}_3} = 3/7$; (b) $V_{\text{DMF}}/V_{\text{CHCl}_3} = 4/6$; (c, d) $V_{\text{DMF}}/V_{\text{CHCl}_3} = 5/5$; (e, f) $V_{\text{DMF}}/V_{\text{CHCl}_3} = 7/3$. The volumes of the aqueous solution and the organic phase are both 5 mL, the concentrations of P3 and AgNO_3 are 0.2 mg mL^{-1} and 0.01 mol L^{-1} , respectively.

The volume ratio of DMF/ CHCl_3 has a crucial influence on the formed microstructures. Although both DMF and CHCl_3 are good solvents for PS-b-P2VP, the polymer exhibits different

self-assembly behavior with different volume ratios of DMF/CHCl₃. For the systems with $V_{\text{DMF}}/V_{\text{CHCl}_3}$ ratios of 3/7, 4/6, and 5/5, multilayer foam structures were observed to form at the air/liquid interface, as shown in Fig. S6. Compared with the 6/4 system, in these cases, more CHCl₃ transferred into the aqueous solution with DMF and started forming droplets once the DMF started diffusing into the water. Here it should be noted that DMF would not be able to diffuse into the water completely, because of the miscibility of DMF and CHCl₃. The PS-*b*-P2VP molecules assembled around the remaining droplets and formed the microcapsules, resulting in the multilayer foam structures at the air/liquid interface. On the other hand, the dissolution of PS blocks in CHCl₃ is conducive to the free dispersion of PS chains, thereby weakening the interaction between the chains, leading to an increase in p . It can be seen in Fig. S6a-c that the size of the microcapsules decreased as the relative concentration of the CHCl₃ in the organic solutions decreased. As described before, nanowires, together with nanospheres and hollow spheres, formed with the 6/4 organic solution, in which case no foam structure appeared, indicating that no microcapsules formed. This could be attributed to the reduced amount of CHCl₃ in the droplet. However, when the volume ratio changed to 7/3, not only did nanowires, nanospheres, and hollow spheres appear in the film, but also a foam structure (Fig. S6e and f)). In this case, the amount of CHCl₃ in the droplet decreased even further. Therefore, the formation of microcapsules seems difficult to understand and we tried to explain the phenomenon as follows. A larger concentration of CHCl₃ causes the PS chains to freely disperse (for the 3/7, 4/6, and 5/5 systems), whereas an appropriate amount of CHCl₃ appears to behave similar to “glue” to hold the PS chains together to form micelle cores (for the 6/4 system). This was a possible consequence of a weakening of the interaction between the PS chains with a reduced amount of CHCl₃ in the droplets, causing the PS chains to become freely dispersed, ultimately resulting in an increase in the value of p and the formation of microcapsules. It was concluded that the composition of the mixed solvent greatly affects the microstructure of the films.

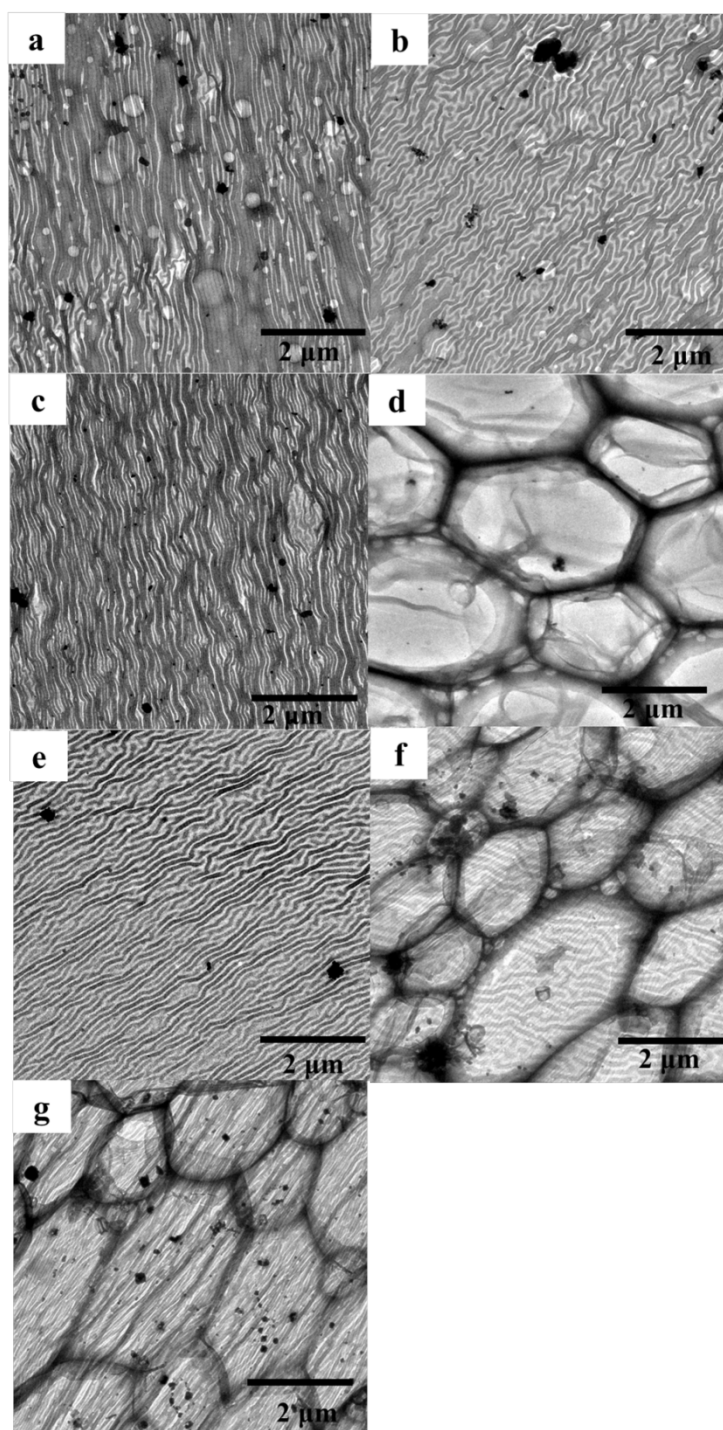


Fig. S7. TEM micrographs of thin films formed at the air/water interface: the volume ratios of the organic and aqueous solutions are 5/2 (a, b), 5/4 (c), 5/10 (d, e), and 5/20 (f, g), respectively. The other parameters are the same as in the typical experiment.

The volume ratios of the organic and aqueous solutions also greatly influenced the formation

of microstructures. As shown in Fig. S7a and b, when the volume ratio was 5/2, nanowires and nanorods formed at the interface. In addition, holes appeared in the background film formed through Gibbs adsorption. In this case, a smaller amount of the organic solution transferred into the aqueous solution in comparison with the typical condition, because only 2 mL aqueous solution was used as the upper phase. Thus, there were insufficient numbers of PS-*b*-P2VP molecules in the aqueous solution. When the volume ratio was 5/4, the nanowire structures were similar to the micro/nano-structures for a volume ratio of 5/5 (Fig. S7c). However, besides nanowires, a foam structure formed in the film with a volume ratio of 5/10 (Fig. S7d and e). For the 5/20 system, nanowires coexisted with foam in the film (Fig. S7f and g)). In these two cases, a large amount of organic solution entered the water phase rapidly and large numbers of cylindrical micelles formed. The formation of these micelles led to the rapid consumption of a large amount of polymer molecules. The depletion of the polymer molecules was possibly faster than the diffusion of DMF; thus, the polymer molecules self-assembled into microcapsules around the DMF droplets, resulting in the formation of foam structures.

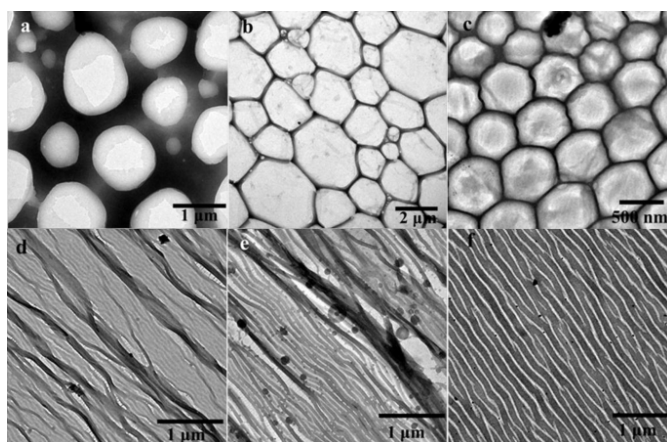


Fig. S8 TEM micrographs of composite thin films formed at the air/water interface by P0 (a), P1 (b), P2 (c,d), P3 (e), and P4 (f). P0 refers to the homopolymer P2VP with M_n of 5300 g mol⁻¹; P1, P2, P3, and P4 refer to PS-*b*-P2VP with different M_n values for the PS and P2VP blocks of 7500/12500, 30000/12500, 110000/12500, and 440000/20000 g mol⁻¹, respectively. The other parameters were the same as for the typical condition.

This approach to fabricating composite thin films would also be suitable for some other polymers. A homopolymer P2VP and block copolymers PS-*b*-P2VP with different molecular

structures were tested here. The length of the P2VP blocks in these block copolymers is equal or close to that of P3, while the length of the PS block changes. Fig. S8 shows the TEM images of the formed films. For P2VP, a foam film composed of isolated microcapsules formed. The templating assembly of P2VP molecules around the organic droplets should lead to the formation of microcapsules. The driving force behind the formation of micelles is known to be hydrophobic interaction. P1 has a much shorter hydrophobic chain than P3. The weak interaction between the PS chains inhibits the formation of micelles. Hence, the polymer molecules assembled around the droplets to form microcapsules adsorbed at the air/water interface to eventually form the foam. Interestingly, two kinds of morphologies, *i.e.*, foam structures and nanowires, appeared simultaneously for P2, as exhibited in Fig. S8c and d. The hydrophobic chain length of P2 is between that of P1 and P3; therefore, two kinds of structures formed. P4 has a longer hydrophobic chain than P3; thus, the interaction between the PS blocks is very strong, resulting in the formation of nanowires. The average diameters of the nanowires formed by P2, P3, and P4 were measured to be 35, 52, and 77 nm, respectively. Composite thin films with various morphologies can be fabricated using this method, and the morphologies can easily be tuned.

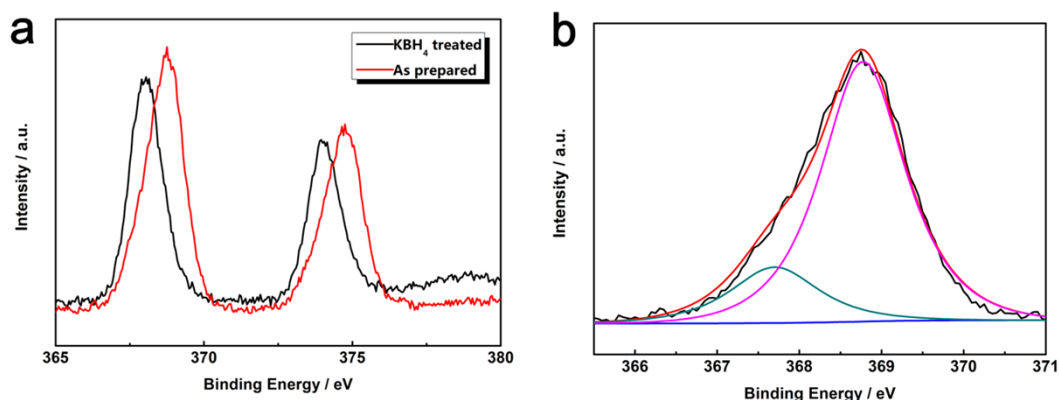


Fig. S9. XPS curves of the composite film prepared before and after KBH_4 aqueous solution treatment, where (b) represents the decomposition curve before treatment.

The composition of the film P3/Ag prepared under the typical experimental conditions was verified using XPS, as shown in Fig. S9. Two bands appeared between 366 and 376 eV, corresponding to $\text{Ag } 3d_{5/2}$ and $\text{Ag } 3d_{3/2}$, respectively. These bands were asymmetric with a

shoulder. Each band was therefore decomposed into two peaks. For the band of Ag $3d_{5/2}$, two peaks at 367.7 and 368.8 eV were obtained, corresponding to Ag(I) and Ag(0), respectively. This indicated that Ag⁺ and Ag(0) coexisted in the as-prepared film. The binding energy of Ag(0) is much higher than 368.0–368.3 eV, which is the binding energy of Ag(0) in the bulk phase,^{1,2} indicating the formation of nanoclusters.³ It can be also seen that the relative content of Ag(0) is much more than that of Ag(I), suggesting that a large proportion of the Ag⁺ ions were reduced by DMF during the assembly process. After treatment with an aqueous solution of KBH₄, two peaks appeared at 368.0 and 374.0 eV, corresponding to the $3d_{5/2}$ and $3d_{3/2}$ levels of Ag(0), respectively. Ag nanoparticles were formed after reduction of Ag⁺ ions. The binding energy 368.0 eV of Ag(0) indicates the formation of larger nanoparticles due to the growth and fusion of the nanoclusters.^{4,5}

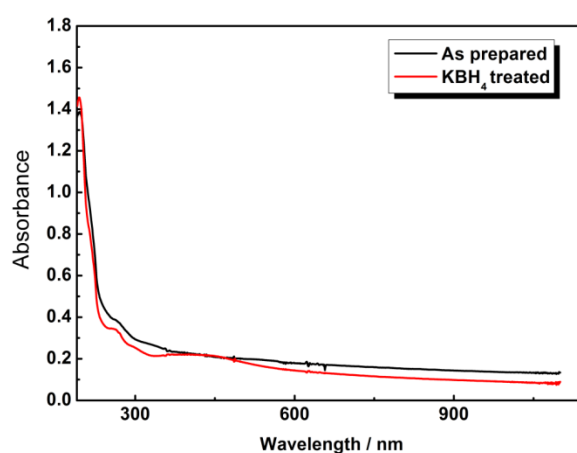


Fig. S10. UV–vis spectra of the thin film obtained at the air/water interface and the film treated with KBH₄ aqueous solution.

Fig. S10 shows the UV–vis spectra of the as-prepared thin films and those treated with an aqueous solution of KBH₄. The as-prepared film has an absorption curve of which the intensity increased steadily from 1000 to 300 nm without the appearance of a surface plasmon resonance band, suggesting the formation of Ag nanoclusters. After treatment, a broader band centered at 420 nm appeared, indicating the formation of larger Ag nanoparticles.^{6,7} These results are in accordance with the TEM observations.

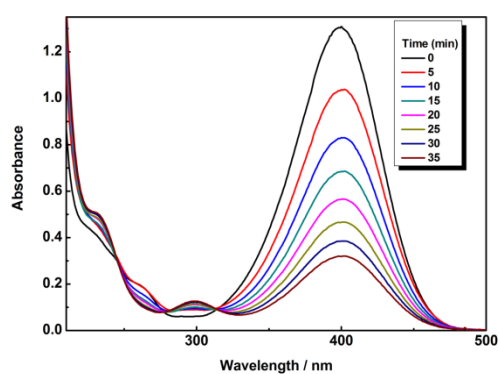


Fig. S11. Catalytic reduction of 4-NP to 4-AP. Time-dependent absorption spectra of the reaction solution in the presence of a composite thin film as catalyst, formed under the typical conditions, and after treatment with an aqueous solution of KBH_4 .

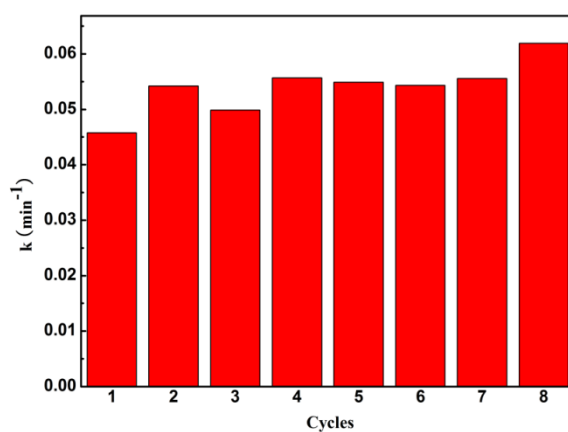


Fig. S12. Apparent rate constants of the reaction in eight successive cycles.

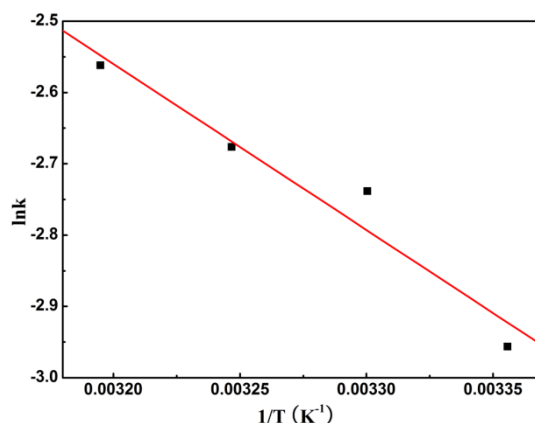


Fig. S13. Arrhenius plot of the apparent rate constants vs $1/T$.

Composite films containing nanowires were doped with Ag nanoclusters. These composites are anticipated to have high catalytic activity for selected heterogeneous catalytic reactions, such as the reduction of 4-NP. Fig. S11 exhibited the time-dependent absorption spectra of the reaction solution in the presence of a composite thin film at 313 K. It is clear that the intensity of the peak at 400 nm quickly decreased and that a new peak appeared at 300 nm. This indicated that the 4-NP was reduced to 4-AP, a reaction which is regarded to be a pseudo-first-order reaction. The apparent rate constant was obtained from the slope of the linear fitted $\ln(A_t/A_0) \sim t$ line. The apparent rate constants obtained when using the composite film as catalyst are shown in Fig. S12. The k values are in close proximity to each other, indicating that the thin film is stable and can be reused. The activation energy E_a of the catalytic reaction was calculated to be 67.5 kJ mol^{-1} (25 – 40 °C) based on the Arrhenius equation, as illustrated in Fig. S13.

3. References for supporting information

- 1 J. F. Weaver and G. B. Hoflund, *J. Phys. Chem.* 1994, **98**, 8519.
- 2 L. H. Tjeng, M. B. J. Meinders, J. van Elp, J. Ghijsen and G. A. Sawatzky, *Phys. Rev. B* 1990, **41**, 3190.

- 3 Y. Liu, L. Chen, Y. Geng, Y.-I. Lee, Y. Li, J. Hao and H.-G. Liu, *J. Colloid Interface Sci.* 2013, **407**, 225.
- 4 A. Murugadoss and A. Chattopadhyay, *J. Phys. Chem. C* 2008, **112**, 11265.
- 5 X. Huang, C. Guo, J. Zuo, N. Zheng and G. D. Stucky, *Small* 2009, **5**, 361.
- 6 J. T. Petty, J. Zheng, N. V. Hud and R. M. Dickson, *J. Am. Chem. Soc.* 2004, **126**, 5207.
- 7 Z. Shen, H. Duan and H. Frey, *Adv. Mater.* 2007, **19**, 349.